Mean Pressure Gradient Prediction Based on Chest Angular Movements and Heart Rate Variability Parameters*

Arash Shokouhmand, *Student Member, IEEE*, Chenxi Yang, *Member, IEEE*, Nicole D. Aranoff, *M.D.*, Elissa Driggin, *M.D.*, Philip Green, *M.D.*, Negar Tavassolian, *Senior Member, IEEE*

Abstract— This study presents our recent findings on the classification of mean pressure gradient using angular chest movements in aortic stenosis (AS) patients. Currently, the severity of aortic stenosis is measured using ultra-sound echocardiography, which is an expensive technology. The proposed framework motivates the use of low-cost wearable sensors, and is based on feature extraction from gyroscopic readings. The feature space consists of the cardiac timing intervals as well as heart rate variability (HRV) parameters to determine the severity of disease. State-of-the-art machine learning (ML) methods are employed to classify the severity levels into mild, moderate, and severe. The best performance is achieved by the Light Gradient-Boosted Machine (Light GBM) with an F1-score of 94.29% and an accuracy of 94.44%. Additionally, game theory-based analyses are employed to examine the top features along with their average impacts on the severity level. It is demonstrated that the isovolumetric contraction time (IVCT) and isovolumetric relaxation time (IVRT) are the most representative features for AS severity.

Clinical Relevance— The proposed framework could be an appropriate low-cost alternative to ultra-sound echocardiography, which is a costly method.

I. INTRODUCTION

Cardiovascular diseases (CVD) have remained the leading cause of death at the global level for the past 20 years [1]. Valvular heart diseases (VHD) are among the most prevalent CVDs, accounting for up to 20% of all surgical procedures in the United States [2]. A highly common VHD in developed countries, aortic stenosis (AS), is defined as the narrowing of the aortic valve opening [3]. Severe aortic stenosis is associated with a progressive cardiac remodeling, e.g., hypertrophy, which ultimately leads to heart failure and death, unless the valve is replaced [4]. Therefore, a precise assessment of the severity of stenosis allows for patient management and risk stratification. Echocardiography is the main method to grade AS severity. Mean pressure gradient (MPG) is one of the echocardiography parameters that are concordant with the severity level of the disease, and is defined as the difference in blood pressure between the left

ventricle and the aorta [4]. Yet, echocardiography monitoring is expensive and limited to use in the clinic. On the other hand, wearable sensor technologies, such as electrocardiography (ECG), offer non-invasive and low-cost measurements of biological signals. Cardio-mechanical signals, representing the linear and angular chest movements induced by the heart activity, can be measured using micro-electromechanical accelerometers gyroscopes, and system (MEMS) respectively. The linear and the angular vibrations are called seismo-cardiography (SCG) and gyro-cardiography (GCG) signals, respectively. These modalities have been used for diagnosing various types of CVD in the literature [5], [6].

Our research group has previously conducted studies on the detection of CVDs using SCG and GCG signals. For instance in [7], general heart rate abnormality was discussed through the morphological changes occurring in cardio-mechanical signals, where an accuracy of 99.5% was reported. Additionally, we employed SCG/GCG signals to diagnose aortic stenosis using time-frequency characteristics of the signals, where a random forest classifier predicted the existence of AS by 97.43% of accuracy [8]. Furthermore, adopting continuous wavelet transform and deep learning algorithms, a classification framework was proposed for AS detection based on multi-dimensional SCG and GCG signals, which was capable of diagnosing AS with 98.00% of F1-score [9]. Furthermore, patients were classified 96.00% correctly through the SCG/GCG signals acquired from their chest movements into three types of CVD, with which they had been diagnosed.

In this study, we propose a wearable sensor-based method for classifying the severity of aortic stenosis. This method involves chest angular movements recorded by gyroscopes as well as heart rate variability (HRV) parameters calculated from peak-to-peak intervals of the GCG signal. As mentioned earlier, the measurement of the mean pressure gradient (MPG) across the aortic valve provides significant information about the severity of aortic stenosis [4]. On the other hand, cardiac timing intervals and HRV parameters have been shown to change with abnormalities in the cardiac

Chenxi Yang is an Associate Professor at the School of Instrument Science and Engineering at Southeast University, Nanjing, Jiangsu, China.

Nicole D. Aranoff is at the Department of Cardiovascular Medicine at Mount Sinai Morningside Hospital, New York, NY, USA.

Elissa Driggin is at the New York-Presbyterian Hospital and Columbia University Irving Medical Center, New York, NY, USA.

Philip Green is an interventional cardiologist at the Department of Cardiovascular Medicine at Mount Sinai Morningside Hospital, New York, NY, USA.

Negar Tavassolian is an Associate Professor at the Department of Electrical and Computer Engineering at Stevens Institute of Technology, Hoboken, NJ 07030, USA.

^{*} Research was supported by National Science Foundation (NSF) under award number 1855394.

Arash Shokouhmand is a Ph.D. student at the Department of Electrical and Computer Engineering at Stevens Institute of Technology, Hoboken, NJ 07030, USA. (e-mail: ashokouh@stevens.edu).

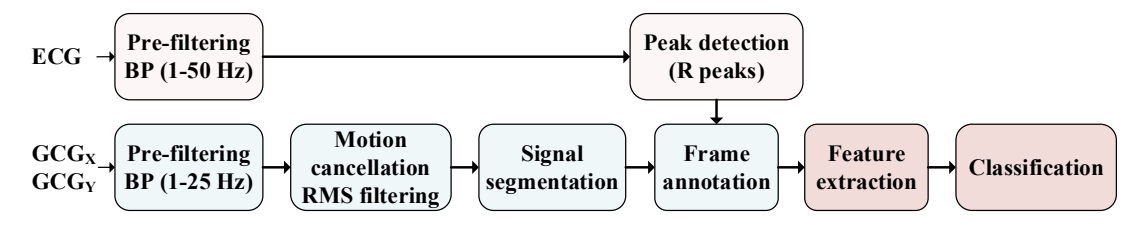


Fig. 1. Signal processing, feature extraction, and classification flow graph proposed in this work.

activity [10]. Hence, this paper targets a meaningful connection between MPG readings from echocardiography and the extracted features from GCG. To the best of our knowledge, this is the first study addressing the classification of severity level in AS through machine learning (ML) methodologies.

The rest of the paper is organized as follows. In Section II, we describe the experimental protocols, the data acquisition procedure, the feature extraction methods, and the predictive models. Experimental results are presented and discussed in Section III, while the paper is concluded in Section IV.

II. METHODOLOGY

A. Experimental Setup and Data Acquisition

This study includes thirty-two AS patients (sixteen males and sixteen females). The average (standard deviation) age of the patients is 84.18 (9.61) years, where eleven, twelve, and nine patients are respectively diagnosed with mild (MPG < 30 mm Hg), moderate (30 < MPG < 50 mm Hg), and severe AS (MPG > 50 mm Hg), respectively.

Angular vibrations of the chest wall were recorded using a commercial wearable sensor node (Shimmer3 from Shimmer sensing) secured by a band strap on the mid-sternum along the third rib. A three-axis gyroscope records the GCG signal in three dimensions. The *X, Y,* and *Z* axes correspond to the shoulder-to-shoulder, head-to-toe, and dorso-ventral directions, respectively. In this paper, the dimensional letters *X, Y,* and *Z* appended as sub-scripts to GCG will denote the signal from the corresponding axis, respectively. Simultaneously, a four-lead ECG sensor was used as the

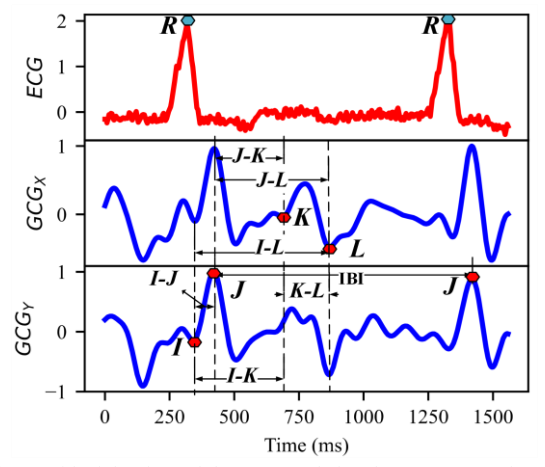


Fig. 2. Fiducial points of the measured signals. From top to bottom: ECG, GCG_X , and GCG_Y .

reference to record the electrical activity in the heart. All waveforms were recorded at a sampling rate of 256 Hz. Immediately after, the heart rhythm and valve parameters such as MPG were also measured by an ultrasound echocardiography machine.

All data were collected at the cardiac care unit of the Columbia University Medical Center (CUMC). The subjects were seated at rest on a bed for at least five minutes. They breathed naturally without controlling their breathing depths. The patient experimental protocol was approved by the Institutional Review Board of CUMC under protocol number AAAR4104. The collected data were transferred to a computer and processed in a Python framework. The step-bystep flow graph of the developed framework for preprocessing, feature extraction, and classification is illustrated in Fig. 1.

B. Signal Pre-processing

Firstly, to remove baseline wandering and noise artifacts, GCG_X and GCG_Y signals were band-pass filtered using a 4thorder Butterworth filter over the range of 1-20 Hz, as shown in Fig. 1. The simultaneously-recorded ECG channels were band-pass filtered retaining the frequency components within the range of 1-50 Hz. Subsequently, motion artifacts associated with movements during recordings were removed from GCG signals by applying a root-mean-square (RMS) filter with a sliding window of 500 ms for signal segmentation. The segment removal threshold was selected as twice the median value of the filter. It should be mentioned that after motion artifact removal, the remaining segments were attached to each other only if there was no discontinuity between the consecutive 500-ms segments. The resulting large segments were segmented into 10-second time frames with 80% overlap between consecutive frames. For every 10second frame, the R-peaks in the ECG signal were detected by the Pan-Tompkin algorithm [11]. The GCG frames were then annotated with I, J, K, and L points, using the R-peaks according to the methods proposed in the literature [12]. An example of the annotation is depicted in Fig. 2.

C. Feature Extraction

The fiducial points on GCG signals are expected to provide valuable information about the function of the cardiovascular system [12]. Once GCG signals were annotated, two types of features were extracted from each frame: time-domain HRV parameters and GCG timing intervals.

TABLE I. PERFORMANCE EVALUATION OF THE ML TECHNIQUES USED IN THIS WORK

Classifier	Performance (%)			
	Accuracy	Precision	Recall	F1-score
DT	58.68	73.26	55.21	52.77
RF	75.17	78.19	73.86	74.98
SVM	83.33	83.64	82.44	82.85
XGBoost	93.75	93.80	93.51	93.64
CatBoost	93.75	93.71	93.44	93.57
LightGBM	94.44	94.45	94.17	94.29

1) Time-domain HRV parameters: Time-domain HRV parameters provide valuable information about cardiac activity [13]. For temporal HRV parameters, a few timedomain analyses were applied to the series of successive interbeat intervals (IBIs). The normal-to-normal IBI (NN) is defined as the interval between consecutive I peaks in the GCG signals [14]. A few HRV features were extracted from the NN time series, such as the average (AVNN), standard (SDNN), root-mean-square of successive deviation differences (RMSSD), and proportion of the number of adjacent NN intervals whose durations differ more than 50 ms (NN50) to the total number of NNs (pNN50). It is worth mentioning that SDNN, RMSSD, and pNN50 are of great clinical importance as they allow for measuring cardiac risk, respiratory arrhythmia, and parasympathetic nervous activity [13], [15]. Additionally, we added the median, skewness, kurtosis, entropy (ENN), self-entropy (SENN), and conditional entropy (CENN) values of NNs to our designed Due to the nonlinearity underlying the feature space. dynamics of HRV, we also extracted the vector angular index (VAI), the vector length index (VLI), SD1, and SD2 out of the Poincare map - a scatter plot of NN at time t in terms of NN at time t+1 [16].

2) GCG timing intervals: A few timing interval parameters describing the cardiac system were calculated for the GCG signal. It has been demonstrated that the isovolumetric contraction time (IVCT), isovolumetric relaxation time (IVRT), and left ventricular ejection time (LVET) are correlated with I-J, L-K, and K-J, respectively [17]. Other parameters such as the intervals between each pair of the fiducial points depicted in Fig. 2 along with their mean, median, standard deviation, skewness, and kurtosis values were also extracted as auxiliary features. The logic behind such an exhaustive feature extraction is to characterize the most relevant GCG timing intervals resulting in the highest accuracy for determining the severity level of AS.

D. Predictive Methods

Predictive models which are employed in this study consist of decision tree (DT), random forest (RF), support vector machine (SVM), extreme gradient boosting (XGBoost) [18], categorical boosting (CatBoost) [19], and light gradient-boosted machine (LightGBM) [20]. These models are selected as they are expected to work properly with respect to the sample space size prepared in this work. All methods except SVM are based on decision tree. The last three

classifiers exploit the gradient boosting mechanism in order to minimize the prediction error, although they differ in terms of feature splitting techniques. Another reason for choosing the above-mentioned methods is to make a comparison in terms of their performance in the context of cardiomechanical signals.

According to the severity levels mentioned earlier, a three-class dataset is provided. The dataset is trained for all the classifiers and evaluated using a validation set. Firstly, the dataset is split into two parts, training (80.00%) and test (20.00%) datasets. Then, the training dataset is fed to the predictive models, where hyperparameters are tuned in a 10-fold cross-validation (10-CV) practice. In the end, the trained models are evaluated against the test dataset to assess the robustness and generalizability of the trained models on an unseen dataset.

III. EXPERIMENTAL RESULTS

In this section, the details of the experiments are comprehensively discussed. A total of 2,878 signal frames were divided into two parts; 2,302 frames (equivalent to 25 subjects) were used for training, and the remaining 576 frames (equivalent to 7 subjects) constituted the test set. At every fold of 10-CV, the model is trained on 2,072 frames, and tested on the remaining 230 frames to optimize the hyperparameters. In the remainder of the paper, the performance evaluation is reported on the unseen dataset, i.e., the test dataset.

A. Performance Evaluation

In this section, the performance of the proposed framework is evaluated by applying the models on the test dataset. Next, by comparing the predicted values and the true labels, the performance of the methods are reported using standard metrics such as accuracy, precision, recall, and F1-score. Table I summarizes the performance results of the predictive models introduced in the previous section. The best performance is reported by 94.44% accuracy, 94.29% F1-

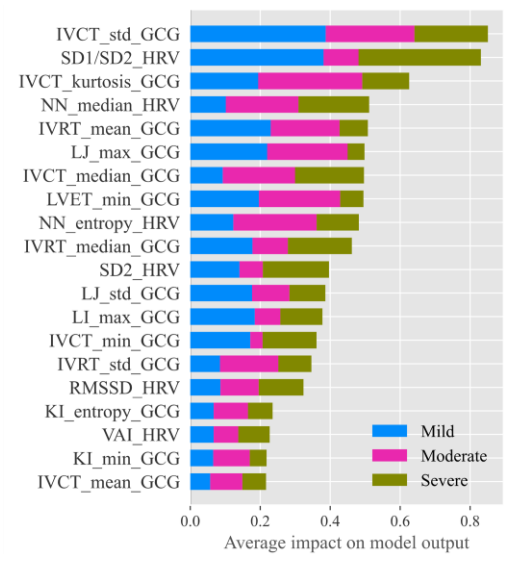


Fig. 3. Top features for AS severity classification and their average impact on the class score ranked by Light GBM.

score, 94.45% precision, and 94.17% recall for LightGBM. The XGBoost is the runner-up predictive model that could predict the severity level by 93.75% accuracy, 93.71% F1score, 93.64% precision, and 93.51% recall, quite close values to LightGBM. As such, the proposed framework is indicated to be sufficiently capable of classifying the severity level of stenosis from GCG readings. As expected, gradient-based boosting methods outperform other simpler tree-based algorithms such as DT and RF, whereas SVM leveraging a hinge loss could predict the severity level by 83.33% accuracy. This indicates the superiority of state-of-the-art tree-based methods over SVM. Furthermore, CatBoost shows almost the same performance as XGBoost in spite of its higher complexity in the feature splitting procedure. Having analyzed the reported performance, it is concluded that the proposed feature space highly correlates with the severity level of aortic stenosis, which is a promising achievement.

B. Top Features

A significant point that discriminates the tree-based methods from other machine learning techniques is their interpretability in terms of performance. This means that the top features, best representing the outcome, could be determined using feature importance scores. The f-scores provided by the gradient-based models consider the impacts of the entire samples on the output. In this work, however, we found the top features using the Shapley Additive exPlanations (SHAP) technique, a game theory-based approach for interpreting the output of a model in terms of the input feature space. SHAP calculates the feature importance in terms of the impact of every single observation on the output [21]. Fig. 3 demonstrates the average impact of the top 20 features on the model output. As illustrated, six features from HRV parameters and fourteen features from GCG timing intervals constitute the top features. IVCT and IVRT that correspond to ventricles iso-volumetrically contraction time and the time interval between aortic valve closure and the onset of the opening of mitral valve, respectively, hold the highest frequencies among the top GCG intervals. Among the top HRV features, three are listed from the Poincare characteristic, whereas the remaining are from the typical HRV features calculated from NN. Considering the points mentioned above, IVCT, IVRT, and Poincare HRV features are the most correlated features with the severity level of AS.

IV. CONCLUSION

This paper reports on the development of a novel framework for the classification of the severity level of aortic stenosis. The proposed method performs based on the changes in the pattern of angular chest movements induced by the cardiac activity. A large feature space is provided comprising the timing intervals between fiducial points on the GCG signal and time-domain HRV parameters. Machine learning techniques are used to classify the severity associated with stenosis, among which LightGBM outperforms the other classifiers with an F1-score of 94.29%. Furthermore, the top features were ranked using a game theory-based method, namely SHAP, where IVCT and IVRT suggested the top

frequencies among others. This indicates high correlations between the aortic stenosis level and the aforementioned features, which can be further explored in the context of risk management for AS patients in the future.

REFERENCES

- W. H. O. (WHO), "WHO reveals leading causes of death and disability worldwide: 2000-2019," (WHO), World Health Organization, 2020. https://www.who.int/news/item/09-12-2020-who-reveals-leadingcauses-of-death-and-disability-worldwide-2000-2019.
- [2] K. Maganti, V. H. Rigolin, M. E. Sarano, and R. O. Bonow, "Valvular heart disease: diagnosis and management," in *Mayo Clinic Proceedings*, 2010, vol. 85, no. 5, pp. 483–500.
- [3] B. A. Carabello and W. J. Paulus, "Aortic stenosis," *Lancet*, vol. 373, no. 9667, pp. 956–966, 2009.
- [4] J. Ternacle and M.-A. Clavel, "Assessment of aortic stenosis severity: a multimodality approach," *Cardiol. Clin.*, vol. 38, no. 1, pp. 13–22, 2020.
- [5] O. T. Inan et al., "Novel wearable seismocardiography and machine learning algorithms can assess clinical status of heart failure patients," Circ. Hear. Fail., vol. 11, no. 1, p. e004313, 2018.
- [6] T. Hurnanen et al., "Automated detection of atrial fibrillation based on time-frequency analysis of seismocardiograms," *IEEE J. Biomed. Heal.* informatics, vol. 21, no. 5, pp. 1233–1241, 2016.
- [7] C. Yang, N. D. Aranoff, P. Green, and N. Tavassolian, "A binary classification of cardiovascular abnormality using time-frequency features of cardio-mechanical signals," in 2018 40th Annual International Conference of the IEEE Engineering in Medicine and Biology Society (EMBC), 2018, pp. 5438–5441.
- [8] C. Yang, N. D. Aranoff, P. Green, and N. Tavassolian, "Classification of Aortic Stenosis Using Time-Frequency Features From Chest Cardio-Mechanical Signals.," *IEEE Trans. Biomed. Eng.*, vol. 67, no. 6, pp. 1672–1683, 2020.
- [9] C. Yang, B. D. Ojha, N. D. Aranoff, P. Green, and N. Tavassolian, "Classification of aortic stenosis using conventional machine learning and deep learning methods based on multi-dimensional cardiomechanical signals," Sci. Rep., vol. 10, no. 1, pp. 1–11, 2020.
- [10] J. Jung et al., "Factors influencing heart rate variability in patients with severe aortic valve disease," Clin. Cardiol., vol. 20, no. 4, pp. 341–344, 1997
- [11] J. Pan and W. J. Tompkins, "A real-time QRS detection algorithm," IEEE Trans. Biomed. Eng., no. 3, pp. 230–236, 1985.
- [12] M. J. Tadi et al., "A real-time approach for heart rate monitoring using a Hilbert transform in seismocardiograms," *Physiol. Meas.*, vol. 37, no. 11, p. 1885, 2016.
- [13] F. Shaffer and J. P. Ginsberg, "An overview of heart rate variability metrics and norms," Front. public Heal., vol. 5, p. 258, 2017.
- [14] S. Sieciński, P. S. Kostka, and E. J. Tkacz, "Heart Rate Variability Analysis on Electrocardiograms, Seismocardiograms and Gyrocardiograms on Healthy Volunteers," *Sensors*, vol. 20, no. 16, p. 4522, 2020.
- [15] U. R. Acharya, K. P. Joseph, N. Kannathal, C. M. Lim, and J. S. Suri, "Heart rate variability: a review," *Med. Biol. Eng. Comput.*, vol. 44, no. 12, pp. 1031–1051, 2006.
- [16] M. Brennan, M. Palaniswami, and P. Kamen, "Do existing measures of Poincare plot geometry reflect nonlinear features of heart rate variability?," *IEEE Trans. Biomed. Eng.*, vol. 48, no. 11, pp. 1342– 1347, 2001.
- [17] M. J. Tadi et al., "Gyrocardiography: A new non-invasive monitoring method for the assessment of cardiac mechanics and the estimation of hemodynamic variables," Sci. Rep., vol. 7, no. 1, pp. 1–11, 2017.
- [18] T. Chen and C. Guestrin, "Xgboost: A scalable tree boosting system," in Proceedings of the 22nd acm sigkdd international conference on knowledge discovery and data mining, 2016, pp. 785–794.
- [19] L. Prokhorenkova, G. Gusev, A. Vorobev, A. V. Dorogush, and A. Gulin, "CatBoost: unbiased boosting with categorical features," arXiv Prepr. arXiv1706.09516, 2017.
- [20] G. Ke et al., "Lightgbm: A highly efficient gradient boosting decision tree," Adv. Neural Inf. Process. Syst., vol. 30, pp. 3146–3154, 2017.
- [21] S. Lundberg and S.-I. Lee, "A unified approach to interpreting model predictions," arXiv Prepr. arXiv1705.07874, 2017.